Figure 6. Log ($k^{corr}\Gamma$) versus log (D_s) for the data in CH_3-$(OCH_2CH_2)_nOCH_3/LiClO_4$ solvent series (□) at 23 °C (Table I); in DME/$LiClO_4$ (⬚), tetraglyme/$LiClO_4$ (⊗), Me_2PEG-1000/$LiClO_4$ (⊖), and Me_2PEG-2000/$LiClO_4$ (⊕) at 55 °C (Table I); in Me_2PEG-400/$LiClO_4$ (●) and in Me_2PEG-400/$Zn(CF_3SO_3)_2$ (△) at different electrolyte concentrations (Table II); in Me_2PEG-400/$LiClO_4$ (○) at different temperatures (Table III) and in Me_2PEG-400/CH_3CN mixture solutions (■) (ref 1). The lines are drawn only to aid in recognizing different groups of data.

correlated groups: variations in $k^{corr}\Gamma$ and D_s with chain length at 23° (□) and at 55 °C (⊕, ⊖, ⊗, ⬚) form two roughly parallel lines with unity slope, whereas variations in $k^{corr}\Gamma$ and D_s with electrolyte concentration ($LiClO_4$ (●) and $Zn(CF_3SO_3)_2$ (△)),

in Me_2PEG-400/$LiClO_4$ with temperature (○), and in Me_2PEG-400/$LiClO_4$ with added CH_3CN (■, previous data[1]), form individual correlation lines with varied but >1 slopes. While there are clearly subtle controlling effects in relaxation timescales that produce these groupings, the main point is clear; electron-transfer rate, as controlled by dipolar fluctuation rate, and diffusion, as controlled by chain segmental mobility, are within a given set of experimental conditions tightly correlated.

The importance of reaction adiabaticity in controlling the effect of monomer solvent τ_L on reaction rates was pointed out recently by Weaver.[3d] A final comment on this matter is in order since we have recently described[11] electron self-exchange dynamics between tetracyanoquinodimethane and its radical anion that showed a correlation between reaction rate ($k_{ex}\delta^2$) and reactant diffusivity (D_s) reminiscent of the present Figure 6, but occurring over a much larger, (10^5-fold) range. The TCNQ results were interpreted as long-distance electron transfers provoked by a combination of large $TCNQ^{0/-}$ self-exchange rate constant and very slow reactant diffusion rates; this reaction is thus nonadiabatic. It is, on the other hand, relatively easy to show that the diffusion and electron transfer rates of reaction 1 are such that electron transfer is expected to occur at collision contact. Based on this and previous[19] observations, reaction 1 should be reasonably adiabatic in the polyether solvent and the analysis here is not to be confused with the TCNQ case.

Importance of the Anisotropy of Atoms in Molecules for the Representation of Electron Density Distributions with Lewis Structures. A Case Study of Aliphatic Diazonium Ions

Rainer Glaser* and Godwin Sik-Cheung Choy[1]

Contribution from the Department of Chemistry, University of Missouri, Columbia, Missouri 65211. Received March 30, 1992

Abstract: The bond formation between a cation X^+ and an electron donor D is examined as a function of the electron acceptor capability of X^+ with topological electron density analyses at the RHF and MP2 levels. Atom populations *and* atom dipoles are important for the description of dative bond formation. Dative bond formation is manifested primarily in the anisotropy of the donor basin for weak acceptors X while charge transfer becomes important for stronger acceptors. Other population analyses allow for the estimation of *bond polarity* but neglect the importance of *atom polarities*. The different stages of dative bond formation are exemplified by analysis of the electron density distributions of heterosubstituted diazonium ions $(X-N_2)^+$ with different acceptors X and by analysis of charge transfer and of atom anisotropies as a function of progressing X–N bond formation. Various Lewis structures are discussed as representations of the electron density distributions resulting from X–N bonding. The consideration of X–N nonconnected Lewis structures is required to adequately represent the electron density distributions. Atom anisotropies also play an important role for the correct appreciation of electron correlation effects on the basis of integrated atomic properties.

Introduction

Molecular charge distributions play an important role in discussions of bonding and reactivity. Lewis structures are commonly used in these discussions although the *formal* charges in the Lewis structures may not represent the charge distribution correctly. Carbon monoxide is a well-known example. It is thus of great significance to establish relations between the electron density

distribution and the Lewis structures. The consideration of bond polarities based on electronegativity differences or the consideration of different valence bond structures are attempts in this direction, but often it is difficult to reconcile[2] the two descriptions, and their apparent inconsistency has received considerable recent attention.[3] The general task is a difficult one as such a generalization would have to provide for a prescription as to how the electron density

(1) (a) Presented in part at the 25th Midwest Regional Meeting of the American Chemical Society, Manhattan, KS, Nov 1990. (b) Part of the projected Ph.D. dissertation of G. S.-C. Choy.

(2) Glaser, R. *J. Comput. Chem.* **1990**, *11*, 663.
(3) Wiberg, K. B., et al. *J. Am. Chem. Soc.* **1992**, *114*, 831, 841 and references therein.

Lewis Structures of Aliphatic Diazonium Ions

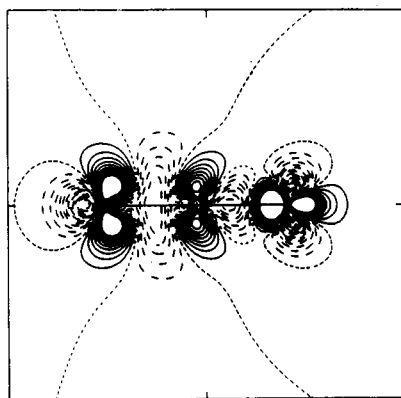J. Am. Chem. Soc., Vol. 115, No. 6, 1993   2341

Figure 1. Surface and contour plots of the electron density difference function $\Delta\rho = \rho(MP2) - \rho(RHF)$ of **1** (F is on the right). Positive areas of $\Delta\rho$ are contoured with solid lines, short dash indicates $\Delta\rho = 0$, and long dashed lines are used to contour negative regions of $\Delta\rho$. Contours start at -0.06 electron au^{-3} and their value is increased in increments of 0.003.

distribution can be interpreted with the Lewis structures and vice versa. A first step in this direction would have to address the representation of electron density distributions with Lewis structures. Here we describe a case study aimed in this direction. Much of our work on deamination reactions has focused on diazonium ions, and they provide an excellent example since the *actual* atom charges deviate significantly from the *formal* charges of the Lewis notations.

Our theoretical studies of C-hybridization effects on the C–N linkages in diazonium ions[4,5] showed that it is the hydrocarbon fragment that carries most of the positive charge while the diazo group is strongly polarized but charged little. A bonding model was proposed that is consistent with their electron density distributions, that also applies to diazonium dications[2] and phenyl diazonium ion,[6] and that was confirmed with electron density analyses at correlated levels.[7] This bonding model was shown to provide an explanation for the incipient nucleophilic attack in diazonium ions with proximate nucleophiles, thereby establishing a crucial link between experiment and theory.[8,9] The atom charges derived from the electron density distributions contrast with those of the commonly used Lewis notations **A** for diazonium ions.[10] Representation by **A** appears inadequate as it assigns not only a positive charge to the N_2 group as a whole but also assigns this charge to N_α which features as the negative end of the internal N_2 dipole in the density model. Lewis structure **B** suffers only from the first of these disadvantages. **C** usually is assigned little importance but it might become important if X has lone pairs available for donation.

X———N$^+$≡≡N | X———N̄===N$^+$| X$^+$===N$^+$===N̈

A   **B**   **C**
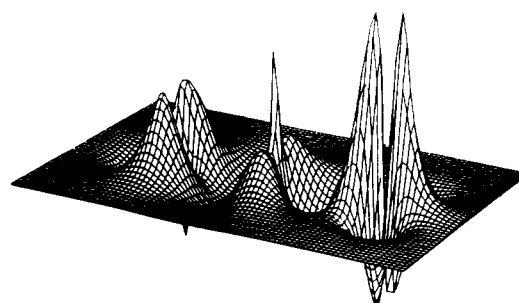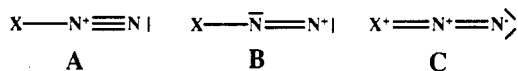
To further probe the nature of the bonding in aliphatic diazonium ions and to address the relation between their electronic structures and the Lewis notation, we have studied the fluoro- (**1**), the hydroxy- (**2**), and the amino- (**3**) diazonium ions in comparison to methyldiazonium ion (**4**). While **1** is known[11,12] and well characterized,[13–15] **2** is still elusive,[16,17] but there is evidence for its intermediacy in the diazoniation of hydroxylamine and the closely related methoxydiazonium ion CH_3ONN^+ is known.
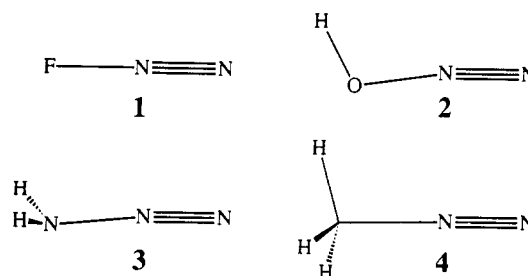
Aminodiazonium ions were originally postulated by Schmidt,[18] and its unequivocal formation and characterization were achieved by Olah's group.[19] More recently, Cacace et al.[20] measured the gas-phase acidity of **3**, and derivatives of **3** have been invoked as intermediates in the intramolecular Schmidt reaction.[21] Alkyldiazonium ions play an important role in deamination reactions[22] that are pertinent to synthetic organic chemistry as well as to the understanding of toxicological aspects.[23] Results of potential energy surface analyses of the heterosubstituted diazonim ion were reported elsewhere,[24] and the MP2/6-31G* structures of their most stable minima are shown. The electron density

(4) Glaser, R. *J. Phys. Chem.* **1989**, *93*, 7993.

(5) For recent theoretical work on aliphatic diazonium ions, see also: (a) Sapse, A.-M.; Allen, E. B.; Lown, J. W. *J. Am. Chem. Soc.* **1988**, *110*, 5671. (b) Ikuta, S. *J. Chem. Phys.* **1989**, *91*, 1376.

(6) Glaser, R.; Choy, G. S.-C.; Horan, C. J. *J. Org. Chem.* **1992**, *57*, 995.

(7) Glaser, R.; Choy, G. S.-C.; Hall, M. K. *J. Am. Chem. Soc.* **1991**, *113*, 1109.

(8) Glaser, R.; Horan, C. J.; Nelson, E.; Hall, M. K. *J. Org. Chem.* **1992**, *57*, 215.

(9) The adequacy of the theoretical models employed for the prediction of structures was demonstrated by our X-ray structure determinations of aromatic and aliphatic diazonium ions. (a) Vinyldiazonium Ions: Glaser, R.; Chen, G. S.; Barnes, C. L. *Angew. Chem.* **1992**, *104*, 749; *Angew. Chem., Int. Ed. Engl.* **1992**, *31*, 740. (b) 2-Carboxybenzenediazonium Chloride Hydrate. Horan, C. J.; Barnes, C. L.; Glaser, R. *Acta Cryst.*, in press. (c) Symmetrically H-Bridged Dimer of 2-Carboxylatobenzenediazonium. The 1:1 Complex between 2-Carboxybenzenediazonium Chloride and 2-Carboxylatodiazonium Zwitterion. Horan, C. J.; Haney, P. E.; Barnes, C. L.; Glaser, R. *Acta Cryst.*, accepted for publication. (d) Crystal Structure of the Explosive Parent Benzyne Precursor: 2-Carboxylatobenzenediazonium Hydrate. Horan, C. J.; Barnes, C. L.; Glaser, R. *Chem. Ber.*, in press.

(10) (a) Elofson, R. M.; Cyr, N.; Laidler, J. K.; Schulz, K. F.; Gadallah, F. F. *Can. J. Chem.* **1984**, *62*, 92. (b) Olah, G. A.; Grant, J. L. *J. Am. Chem. Soc.* **1975**, *97*, 1546.

(11) Review: Laali, K.; Olah, G. A. *Rev. Chem. Intermed.* **1985**, *6*, 237.

(12) Moy, D.; Young, A. R. *J. Am. Chem. Soc.* **1965**, *87*, 1889.

(13) Shamir, J.; Binenboym, J. *J. Mol. Struct.* **1969**, *4*, 98.

(14) Christe, K. O.; Wilson, R. D.; Sawodny, W. *J. Mol. Struct.* **1971**, *8*, 245.

(15) For N-NMR studies of **1**, see: Mason, J.; Christe, K. O. *Inorg. Chem.* **1983**, *22*, 1849.

(16) Hydroxydiazonium ion **3** is more stable than its N-protonated isomer HNNO$^+$: Ferguson, E. F. *Chem. Phys. Lett.* **1989**, *156*, 319.

(17) Olah, G. A.; Herges, R.; Laali, K.; Segal, G. A. *J. Am. Chem. Soc.* **1986**, *108*, 2054.

(18) Schmidt, A. *Chem. Ber.* **1966**, *99*, 2976.

(19) (a) Mertens, A.; Lammertsma, K.; Arvanaghi, M.; Olah, G. A. *J. Am. Chem. Soc.* **1983**, *105*, 5657. (b) Spectroscopy and theory showed that the aminodiazonium ion is favored over the iminodiazenium ion.

(20) (a) Cacace, F.; Attina, M.; Petris, G. De; Grandinetti, F.; Speranza, M. *Gazz. Chim. Ital.* **1990**, *120*, 691. (b) Glaser, R.; Choy, G. S.-C. *J. Org. Chem.* **1992**, *57*, 4976.

(21) Aube, J.; Milligan, G. L. *J. Am. Chem. Soc.* **1991**, *113*, 8965.

(22) Review: Kirmse, W. *Angew. Chem., Int. Ed. Engl.* **1976**, *15*, 251.

(23) For reviews, see Chapters 12–14 in: Chemical Carcinogens; Searle, Ch. E., Ed.; ACS Monograph Ser. 182; American Chemical Society: Washington, DC, 1984; Vol. 2.

(24) Glaser, R.; Choy, G. S.-C. *J. Phys. Chem.* **1991**, *95*, 7682.

Table I. Topological Properties[a,b]

no.[c]	A	B	r_A	r_B	F	ρ	λ_1	λ_2	λ_3	ϵ
					(FNN)[+], **1**					
R,1	N2	N1	0.664	0.408	0.619	0.642	−1.311	−1.311	0.558	0.000
R,2	N2	F3	0.557	0.683	0.449	0.461	−1.212	−1.212	1.184	0.000
M,1	N2	N1	0.642	0.497	0.564	0.532	−0.965	−0.965	0.686	0.000
M,2	N2	F3	0.555	0.700	0.442	0.423	−1.048	−1.048	1.288	0.000
					(HONN)[+], **2**					
R,1	N2	N1	0.660	0.414	0.614	0.651	−1.412	−1.308	0.456	0.079
R,2	N2	O3	0.647	0.622	0.510	0.440	−1.075	−0.957	1.147	0.124
R,3	O3	H4	0.809	0.165	0.831	0.320	−1.892	−1.848	1.606	0.024
M,1	N2	N1	0.544	0.501	0.561	0.543	−1.047	−1.026	0.781	0.020
M,2	N2	O3	0.619	0.652	0.487	0.426	−1.032	−0.922	1.197	0.119
M,3	O3	H4	0.825	0.180	0.821	0.289	−1.557	−1.526	1.474	0.020
					(H$_2$NNN)[+], **3**					
R,1	N2	N1	0.647	0.431	0.600	0.658	−1.503	−1.325	0.345	0.134
R,2	N2	N3	0.778	0.530	0.595	0.374	−0.814	−0.548	0.554	0.484
R,3	N3	H4	0.793	0.214	0.787	0.329	−1.434	−1.377	1.055	0.042
M,1	N2	N1	0.631	0.505	0.555	0.560	−1.138	−1.105	0.753	0.029
M,2	N2	N3	0.722	0.577	0.556	0.383	−0.876	−0.668	0.775	0.310
M,3	N3	H4	0.803	0.223	0.783	0.306	−1.281	−1.237	0.964	0.036

[a] The values r_A and r_B are the distances of the critical point (CP) from atoms A and B (in Å), F is the ratio $r_A/(r_A + r_B)$, ρ is the value of the electron density at the CP (in e au^{-3}, the λ_i are the principal curvatures of ρ at the CP, and the bond ellipticity is derived via $\epsilon = \lambda_n/\lambda_m - 1$, where $\lambda_n < \lambda_m$ and $\lambda_i < 0$. [b] For corresponding data of **4**, see refs 4 and 7. [c] Numbers preceded by "R" and "M" refer to critical points in the RHF/6-31G* and MP2(full)/6-31G* electron densities, respectively.

analysis of the diazonium ions is in the focus of this article, and a variety of methods including basis set partitioning and topological techniques are employed for this purpose. Effects of electron correlation are discussed and dependency on electronegativity is used as the ordering principle.[25] The analysis allows one to determine the relative importance of different canonical Lewis structures. In particular, it is shown that the atomic dipole moments are crucial parameters for the representation of electron density distributions with Lewis structures and also for the interpretation of correlation effects on electron density distributions and their manifestation in the topological parameters.

Computational Methods

As representatives of the basis set partitioning techniques, both Mulliken and Natural Population analyses[26] were employed, and the topological analyses were performed with Bader's theory of atoms in molecules.[27,28] Populations[29] were determined at the RHF and MP2-(full) levels with the 6-31G* basis set.[30] The electron correlation effects on the density are somewhat exaggerated at the MP2 level but agree well with the results of more complete electron correlation methods.[31] The basis set partitioning populations were computed with a version of Gaussian88[32] that included the program NBO.[33,34] The correlated

electron densities were calculated with Firsch's implementation of the Z-vector method.[35] The RHF wave functions and MP2 density matrices were reformatted with the program Psichk[36] and analyzed with Bader's programs Extreme and Proaim.[37] Cross sections of the electron densities were determined with the program Netz,[38] and PV-Wave programs were written for their display. Properties of the integrated atomic moments were analyzed with the program Dipoles.[38]

Results and Discussion

Atom and Fragment Populations. It is highly characteristic for the methyldiazonium ion—and for all alkyl- and aryldiazonium ions and even dications—that the basin of the central nitrogen atom (N$_\alpha$) extends over more than two-thirds of the C-N and over more than half of the N-N bonding regions. This finding can be well described by the F values associated with the N$_\alpha$-X and N$_\alpha$-N$_\beta$ bond critical points (Table I). The N$_\alpha$ basin changes in a characteristic fashion[39] when the alkyl group is replaced by a more electronegative group; the N$_\alpha$ basin extends significantly less into the X-N bonding region but slightly further into the N-N bonding region. This finding is manifested in the RHF as well

diazonium ion	N$_\alpha$-X			N$_\alpha$-N$_\beta$		
	F(RHF)	F(MP2)	$\Delta\rho$	F(RHF)	F(MP2)	$\Delta\rho$
(FNN)[+]	0.449	0.442	−0.038	0.619	0.564	−0.110
(HONN)[+]	0.510	0.487	−0.014	0.614	0.561	−0.108
(H$_2$NNN)[+]	0.595	0.556	+0.009	0.600	0.555	−0.098
(H$_3$CNN)[+]	0.708	0.686	+0.024	0.546	0.537	−0.083

as in the MP2 electron densities. In Figure 1, the electron density difference function $\Delta\rho = \rho(MP2) - \rho(RHF)$ is shown for **1** to

(25) For group electronegativities used here, see: Wells, P. R. *Prog. Phys. Org. Chem.* **1968**, *6*, 111. They are 3.95 (F), 3.70 (OH), 3.35 (NH$_2$), and 2.30 (CH$_3$). Slightly different numerical values are without consequence for our discussion as we use electronegativity merely as an ordering principle and because these values are well correlated with the more recently proposed electronegativity scales by Allen (Allen, L. *J. Am. Chem. Soc.* **1989**, *111*, 9003; **1992**, *114*, 1510) and Boyd et al. (Boyd, R. L.; Edgecombe, K. E. *J. Am. Chem. Chem.* **1988**, *110*, 4182. Boyd, R. J.; Boyd, S. L. *Ibid.* **1992**, *114*, 1652).

(26) Review: Weinhold, F.; Carpenter, J. E. In *The Structure of Small Molecules and Ions*; Naaman, R.; Vager, Z., Eds.; Plenum Press: New York, 1988; p 227ff.

(27) Bader, R. F. W. *Atoms in Molecules. A Quantum Theory*; Oxford University Press: New York, 1990.

(28) Reviews: (a) Bader, R. F. W. *Acc. Chem. Res.* **1985**, *18*, 9. (b) Bader, R. F. W.; Nguyen-Dang, T. T.; Tal Y. *Rep. Prog. Phys.* **1981**, *44*, 893.

(29) For a comparative discussion, see: Glaser, R. *J. Comput. Chem.* **1989**, *10*, 118 and references therein.

(30) (a) Hehre, W. J.; Ditchfield, R.; Pople, J. A. *J. Chem. Phys.* **1972**, *56*, 2257. (b) Hariharan, P. C.; Pople, J. A. *Theor. Chim. Acta* **1973**, *28*, 213. (c) Binkley, J. S.; Gordon, M. S.; DeFrees, D. J.; Pople, J. A. *J. Chem. Phys.* **1982**, *77*, 3654. (d) Six Cartesian second-order Gaussians were used for d-shells.

(31) Wiberg, K. B.; Hadad, C. M.; LePage, T. J.; Breneman, C. M.; Frisch, M. J. *J. Phys. Chem.* **1992**, *96*, 671.

(32) Gaussian88 (Rev. C): Frisch, M. J.; Head-Gordon, M.; Schlegel, H. B.; Raghavachari, K.; Binkley, J. S.; Gonzales, C.; Defrees, D. J.; Fox, D. J.; Whiteside, R. A.; Seeger, R.; Melius, C. F.; Baker, J.; Martin, R. L.; Kahn, L. R.; Stewart, J. J. P.; Fluder, E. M.; Topiol, S.; Pople, J. A. Gaussian, Inc.: Pittsburgh, PA, 1988.

(33) NBO 3.0: Glendening, E. D.; Reed, A. E.; Carpenter, J. E.; Weinhold, F., Theoretical Chemistry Institute and Department of Chemistry, University of Wisconsin, Madison, WI 53706. (b) We thank A. Holder for a copy of this program.

(34) Computations were carried out on a Vaxstation3100, two Vaxstation3520, a network of Silicon Graphics Personal Iris workstations and servers, and on the IBM 4381 and 3090 mainframes of the Campus Computing Center and its attached FPS array processor.

(35) (a) Handy, N. C.; Schaefer, H. F., III *J. Chem. Phys.* **1984**, *81*, 5031. (b) See refs 31 and 32.

(36) Psichk: (a) Lepage, T. J., Department of Chemistry, Yale University, 1988. (b) IBM version by Harris, B., Department of Chemistry, University of Missouri, 1991.

(37) Extreme and Proaim: (a) Biegler-Koenig, F. W.; Bader, R. F. W.; Tang, T. H. *J. Comput. Chem.* **1982**, *3*, 317. (b) Ported to the IBM 4381 by G. Choy and to the Silicon Graphics Personal Iris by R. Glaser.

(38) Netz and Dipoles by Glaser, R., University of Missouri—Columbia, 1990.

(39) For discussions of electronegativity and bond critical point shifts, see: (a) Boyd, R. J.; Boyd, S. L. *J. Am. Chem. Soc.* **1992**, *114*, 1652. (b) Perrin, C. L. *J. Am. Chem. Soc.* **1991**, *113*, 2865 and references therein.

Table II. Integrated Properties[a-c]

atom	RHF/6-31G*				MP2(full)/6-31G*			
	MC	NC	IC	T	MC	NC	IC	T
				1				
N1	0.347	0.432	0.990	53.588 01	0.315	0.369	0.586	54.203 84
N2	0.683	0.541	0.073	54.729 25	0.666	0.574	0.448	54.525 61
F3	−0.030	0.027	−0.062	99.513 84	0.019	0.057	−0.035	99.652 20
Σ	1.000	1.000	1.001	207.831 10	1.000	1.000	0.999	208.381 65
N₂	1.030	0.973	1.063	108.317 26	0.981	0.943	1.034	108.729 45
				2				
N1	0.245	0.393	0.881	53.688 76	0.232	0.328	0.504	54.285 49
N2	0.627	0.414	−0.145	54.896 73	0.588	0.433	0.237	54.717 78
O3	−0.458	−0.412	−0.459	75.067 29	−0.397	−0.370	−0.445	75.293 75
H4	0.586	0.605	0.724	0.263 33	0.577	0.609	0.704	0.271 13
Σ	1.000	1.000	1.001	183.916 11	1.000	1.000	1.000	184.568 15
N₂	0.872	0.807	0.736	108.585 49	0.820	0.761	0.741	109.003 27
HO	0.128	0.193	0.265	75.330 62	0.180	0.239	0.259	75.564 88
				3				
N1	0.110	0.379	0.759	53.799 10	0.126	0.315	0.450	54.323 70
N2	0.426	0.265	−0.387	55.027 14	0.402	0.285	−0.047	54.920 75
N3	−0.540	−0.622	−0.508	54.607 75	−0.520	−0.602	−0.532	54.881 54
H4/5	0.502	0.489	0.568	0.359 72	0.496	0.501	0.565	0.356 56
Σ	1.000	1.000	1.000	164.153 43	1.000	1.000	1.001	164.839 11
N₂	0.536	0.644	0.372	108.826 24	0.528	0.600	0.403	109.244 45
NH₂	0.464	0.356	0.628	55.327 19	0.471	0.399	0.598	55.594 66
				4				
N1	0.139	0.407	0.557	54.003 89	0.154	0.361	0.425	54.347 00
N2	0.194	0.096	−0.397	54.877 29	0.247	0.187	−0.256	55.007 35
C3	−0.320	−0.418	0.264	37.718 47	−0.394	−0.532	0.179	37.940 30
H4	0.329	0.305	0.192	0.538 80	0.331	0.328	0.217	0.521 21
Σ	1.000	1.000	1.000	148.216 03	1.000	1.000	0.999	148.858 28
N₂	0.333	0.503	0.161	108.881 18	0.401	0.548	0.169	39.503 93
CH₃	0.667	0.497	0.839	37.334 85	0.599	0.452	0.830	109.354 34

[a] MC = Mulliken charge, NC = natural charge, and IC = integrated charge. Kinetic energies are in atomic units. T is the integrated kinetic energy corrected for the virial defect of the wave function. [b] Virial ratios $(-V/T)$ of the RHF/6-31G* wave functions: 2.003 024 56 (**1a**), 2.003 264 37 (**2a**), 2.003 221 69 (**3a**), 2.002 775 05 (**4a**), and 2.001 966 33 (**4b**). Virial ratios of the MP2(full)/6-31G*//MP2(full)/6-31G* wave functions: 2.005 276 66 (**1a**), 2.005 793 33 (**2a**), 2.005 806 00 (**3a**), and 2.005 208 61 (**5a**). [c] The differences between Σ T and the directly computed molecule energies are (in kilocalories per mole) at RHF/6-31G* 0.05 (**1**), 0.07 (**2**), 0.00 (**3**), and 0.02 (**4**), and they are at MP2/6-31G* 30.16 (**1**), 90.53 (**2**), 112.87 (**3**), and 120.58 (**4**).

exemplify the effects of electron correlation on the electron density distributions. The effects of electron correlation on alkyldiazonium ions are the results of excitations from the N_σ bonding and nonbonding orbitals into the antibonding N_2 e-orbitals and of a reorganization around X that serves to increase the electron density in the X–C bonding while reducing the density around X perpendicular to the axis. The same patterns are found for **1–3** as well but with quantitative differences. The $\Delta\rho$ values show that electron correlation reduces the density in the N–N bonding region in all cases (and this trend parallels X electronegativity), while it may increase or decrease the density at the X–N bond critical points.

The charges of the N_2 group and of the individual N atoms (Table II) are plotted versus the electronegativity of the X group in Figure 2. We focus first on the results obtained at the correlated level and compare these with the RHF derived values later.[40] All population methods[41] agree that the diazo group essentially carries a full positive charge in **1** and about four-fifths of the positive charge in **2**. The spread in the N_2 charges assigned by the various methods becomes larger for **3** and **4**. The basis set partitioning techniques assign larger positive charges to the N_2 group of **4** (about +0.55) than the density integration technique (+0.17). While all population methods lead to the same conclusion for **1** and **2**, significant qualitative discrepancies occur for the other systems. There is a rough correspondence between the $F(X–N\alpha)$ values, parameters that reflect X–N polarity, and the differences

between the integrated and the basis set partitioning derived charges, but the relation is too rough to be useful even in a semiquantitative way. Different accounting for bond polarity is but one of the factors entering the population differences.

The three population methods agree less with regard to their assignment of the diazo group charge to the central (N_α) and the terminal (N_β) nitrogens.[42] The topological method generally assigns the highest populations to N_α and the lowest to N_β, thereby indicating significant internal polarization within the N_2 group. In **1**, N_β is assigned a charge of +0.59 and N_α carries a charge of +0.45. The charge on N_β depends relatively little on the identity of X; the N_β charge decreases from +0.59 (F) via + 0.50 (OH) and +0.45 (NH₂) to +0.43 (CH₃). Because of this and since the overall charge of the diazo group increases with the electronegativity of X, large variations in the N_α charges result ranging from a significant positive charge of +0.45 for **1** to a negative charge of −0.26 for **4**. The basis set partitioning techniques yield N populations that differ not only in magnitude but also would indicate different N–N bond polarities. The Mulliken analysis, for example, assigns positive charges to *both* N atoms and indicates an increase in the N–N bond polarity with increasing EN(X) where N_α (not N_β) is the more electron deficient atom.

Populations and Lewis Structures. As in the case of the alkyldiazonium ions, the electronic structures of the heterosubstituted derivatives are inconsistent with the commonly used Lewis structure **A** *as the single representation.* While **A** assigns a positive charge to N_α, this work shows that *the positive charge on N_β is always larger than the one on N_α and that N_α might even carry*

(40) We also determined MC and NC values at the RHF/6-31G*// MP2(full)/6-31G* level and found them to deviate but marginally from the RHF/6-31G*//RHF/6-31G* data.
(41) Differences between the analyses were studied at the RHF level: (a) Glaser, R. *J. Comput. Chem.* **1989**, *10*, 118 and references therein. (b) Gronert, S.; Glaser, R.; Streitwieser, A. *J. Am. Chem. Soc.* **1989**, *111*, 3111 and references therein.

(42) Especially for the Mulliken method, the populations also are rather basis set dependent. For example, the RHF/4-31G populations of **2** determined by Olah et al. are 0.42 for N_β and 0.37 for N_α while they are 0.30 (N_β) and 0.56 (N_α) at RHF/6-31G*.
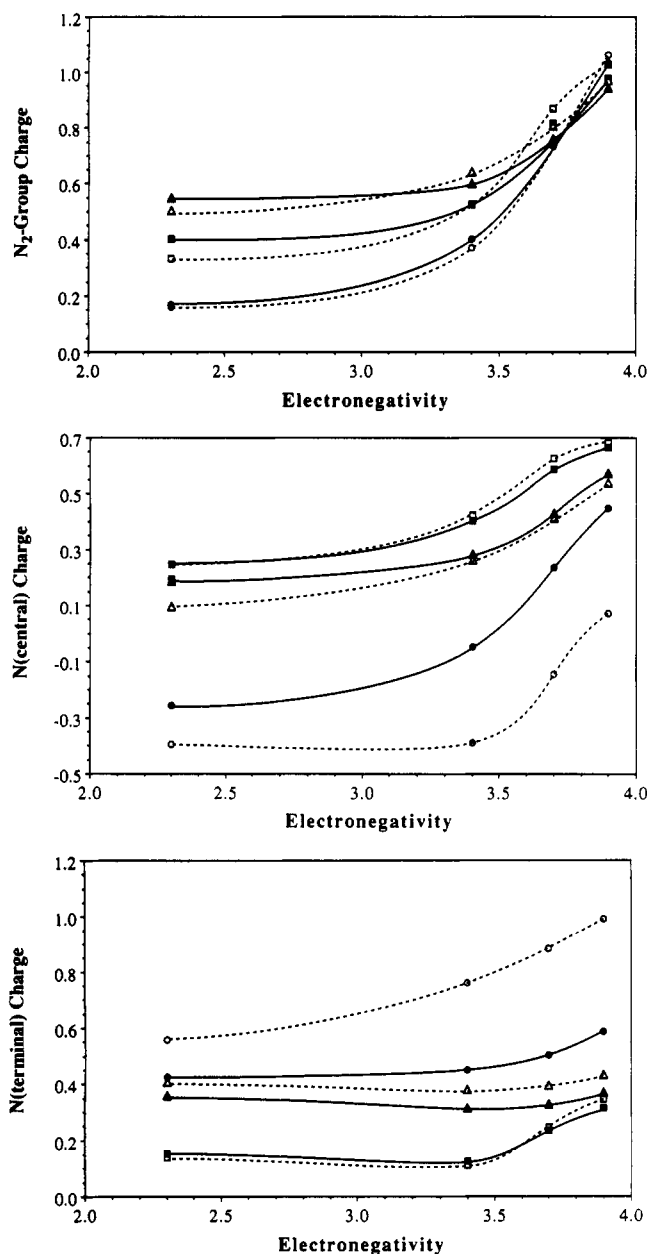
Figure 2. Effect of the X electronegativity on the Mulliken (squares), the natural (triangles), and the integrated charges (circles) of the diazo groups (top), the central N atom (N2, center), and the terminal N atom (N1) in **1 - 4**. Charges derived from the correlated electron density are shown as filled marks with solid lines of interpolation. The unfilled marks and dashed interpolation lines refer to data obtained at the RHF level.

a negative charge. Because of the small charge transfer from the diazo group to the alkyl cation, the X–N bonded Lewis structures **A - C** do not suffice to describe the electron density distribution,
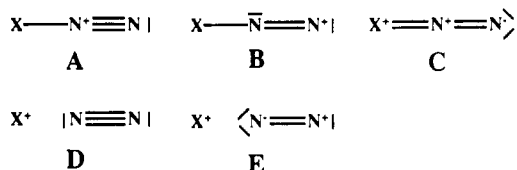
and it becomes imperative to also consider the X–N nonconnected Lewis structures **D** and **E**. Our results suggest that a combination of **D** and **E**[43] best represents the electronic structure of alkyldiazonium ions. As the bond between X and N_α strengthens with increasing electronegativity of X, **A** and **B** (related formally to **D** and **E** by a single shift of an N_α σ electron pair) become more important. In general, those canonical forms that reflect the

Table III. Integrated First Moments[a]

atom	RHF		MP2	
	μ	angle	μ	angle
	Fluorodiazonium Ion			
F	0.0397	180.0	0.0643	180.0
N_{cent}	1.1151	180.0	0.6772	180.0
N_{term}	1.0717	0.0	0.7436	0.0
μ_{mol}	0.2239		0.1330	
	Hydroxydiazonium Ion			
H	0.1048	2.2	0.1085	1.5
O	0.4622	31.3	0.3857	35.5
N_{cent}	0.8222	172.5	0.4905	165.8
N_{term}	1.0594	0.1	0.7601	0.9
μ_{mol}	0.9003		1.0086	
	Aminodiazonium Ion			
H	0.1369	0.5	0.1362	0.3
N_{amino}	0.8043	0.0	0.7174	0.9
N_{cent}	0.3534	168.5	0.1681	152.5
N_{term}	1.0092	0.1	0.7676	0.4
μ_{mol}	1.0354		1.2160	
	Methyldiazonium Ion			
H	0.1242	0.6	0.1305	0.6
C	0.5801	0.0	0.6347	0.0
N_{cent}	0.3029	0.0	0.3839	0.0
N_{term}	0.8124	0.0	0.7060	0.0
μ_{mol}	0.8231		0.8321	

[a] For the diazo nitrogens, the angles are those enclosed between the dipole of one N and the vector toward the other N. For the heteroatoms X and the hydrogens, the angles are those enclosed by the dipole vector of X or H and the vector $X-N_{cent}$ or H–X, respectively. [b] Dipoles are in atomic units: 1 au = 2.5418 D.

polarization of the diazo group in the fashion $N_\alpha{}^{\delta-}-N_\beta{}^{\delta+}$ (**B** and **E**) are more important than those that do not (**A** and **D**). Alkyldiazonium ions and the heteroderivatives differ significantly in that the former essentially are *carbenium* ions whereas the latter are *diazonium* ions with larger positive charges on the *terminal* nitrogen atom. Resonance form **C** contributes little.[44]

D and **E** represent a first approximation to the charge distribution in **4**, but this representation suffers from the disadvantage that it does not clearly express the accumulation of electron density in the C–N bonding region. The more common Lewis structures **A** and **B** would be advantageous in this regard, but they both assign a positive charge to the diazo group which is not compatible with the electron density function. The dilemma can be resolved, however, when both the atom charges *and* the atom dipole moments are considered. The initial phase of dative bond formation is characterized by an increase in the anisotropy of the electron density distribution within the donor basin (which leads to electron density accumulation in the X–N bond), and, importantly, this change in the asymmetry of electron density *might have little effect on the atomic charge but be manifested only in the atomic dipole moments*. Hence, *the evaluation of charges alone will not give an adequate description of the dative bond, but atom anisotropies need to be considered as well*. While the atom charges might indicate **D** and **E**, the anisotropies provide information about the importance of contributions from **A** and **B**. In the following, we report the results of the analysis of the atom anisotropies in **1 - 4**, discuss the progression of atom charges and atom dipole moments along the path of the dative bond formation for the specific case of the hydroxydiazonium ion **2**, and show how the integrated properties of **1 - 4** reflect different degrees of X–N bond formation.

Atom Anisotropy and Intramolecular Polarization. The asymmetry of the electron density function within each basin can be described by the atomic moment μ which is defined[45] as the

(43) We note that the formal electron pair shift leading from **D** to **E** should really be considered as a polarization of both of the N–N π bonds.

(44) The importance of the type **C** structure for **3** had been suggested on the basis of NMR chemical shifts. See ref 19.

F—N≡N

RHF

MP2

HO—N≡N
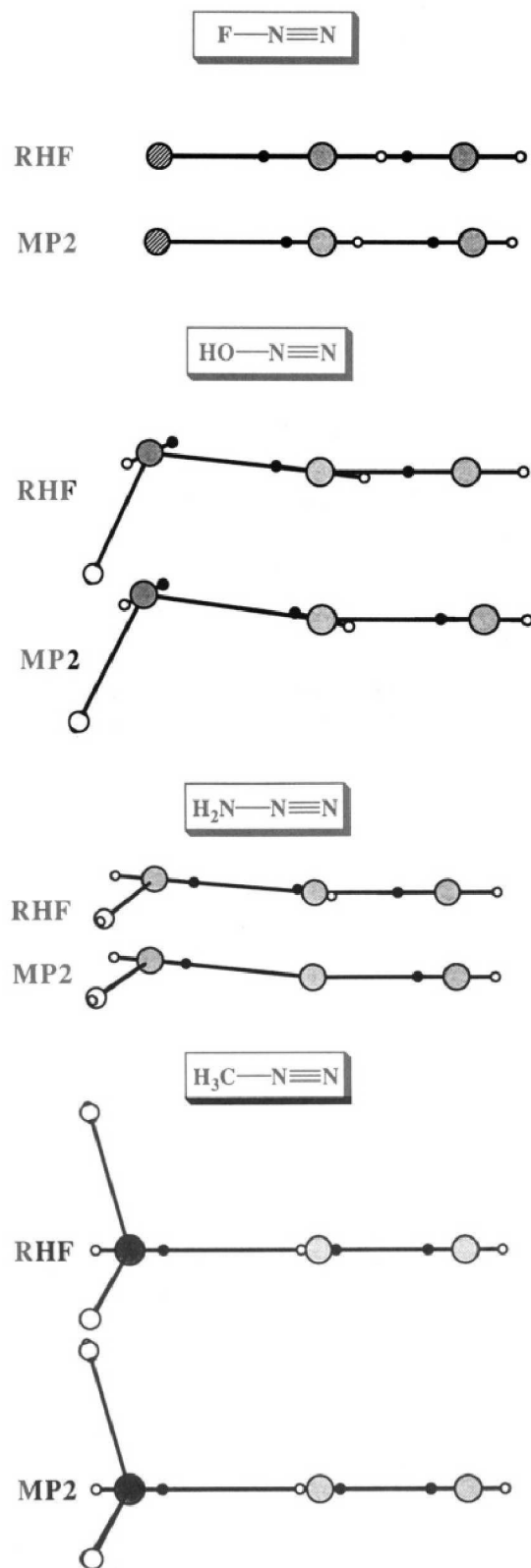
RHF

MP2

H₂N—N≡N

RHF

MP2

H₃C—N≡N

RHF

MP2

Figure 3. The integrated atomic dipole moments are shown superimposed on the molecules as determined at the RHF/6-31G* and MP2(full)/6-31G* levels. Dipoles are directed from the unfilled marks to the filled marks. See Table III for exact angles.

negative of the volume integral of $\mathbf{r}' \rho(\mathbf{r})$ taken over the basin where $\mathbf{r}'$ measures the distance of the position $\mathbf{r}$ from the position of the nucleus Y ($\mathbf{r}' = \mathbf{r} - \mathbf{Y}$). In Figure 3, the μ vectors (O--●) are superimposed on the molecules and they are directed from the
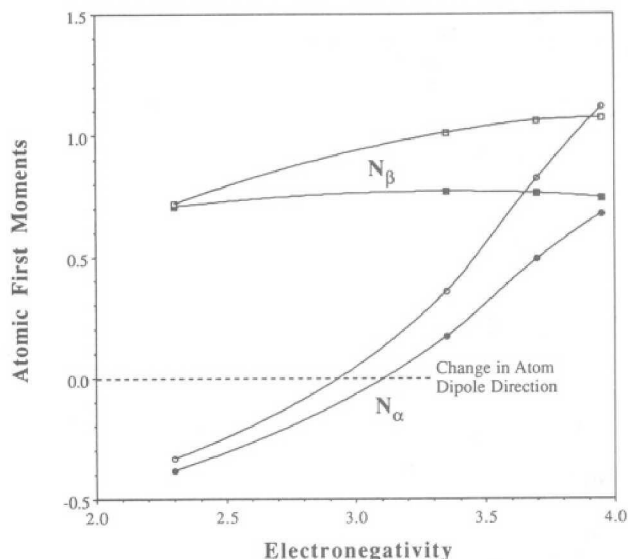
(45) (a) Bader, R. F. W.; LaRouche, A.; Gatti, C.; Carroll, M. T.; MacDougall, P. J.; Wiberg, K. B. *J. Chem. Phys.* **1987**, *87*, 1142. (b) Slee, T. *J. Am. Chem. Soc.* **1986**, *108*, 7541.

Figure 4. Plot of the atomic dipole moments of N_α (circles) and N_β (squares) in the diazonium ions versus the electronegativity of X as determined at the MP2(full)/6-31G* (solid marks) and at the RHF/6-31G* (unfilled marks) levels. The N_β dipoles always point toward N_α, and the N_α dipoles are taken positive if they point away from N_β (parallel to $\mu(N_\beta)$), and negative otherwise.

unfilled "O" to the filled black "●" markers. The absolute values of the dipole moments are given in Table III together with the angles enclosed between μ and the geometrical bond axis. In Figure 4, the effects of electron correlation on the magnitudes of the dipole moments of the diazo nitrogens are shown as a function of the X electronegativity. We will first analyze the dipole moments determined at the correlated level and discuss their relevance for the relation between electron density functions and Lewis structures. We will then discuss how dipole moments are affected by electron correlation and discuss consequences for the interpretation of electron correlation effects on electron density distributions based on integrated properties.

The dipole moments of the terminal N_β atoms always are directed toward N_α. Their values are confined to the comparatively narrow interval of 0.71 to 0.77 atomic unit and they show little dependency on the identity of X. Significantly larger variations occur for $\mu(N_{cent})$ not only in magnitude but also *in their directions*. In **4** and in alkyldiazonium ions in general, $\mu(N_\alpha)$ is directed toward N_β, antiparallel to $\mu(N_\beta)$, and of about half the magnitude of $\mu(N_\beta)$. In the alkyldiazonium ions, the electron density within the basins of N_α and N_β are polarized into the C–N bonding and the N_β lone pair regions, respectively. The directions of these N dipoles are the same as in free[46] N_2 and the changes in magnitude can be understood as the result of polarization induced shifts of the zero-flux surfaces. In going from X = alkyl to the more electronegative X groups, *the dipole moment of N_α reverses its direction and increases in magnitude as the electronegativity increases* (Figures 3 and 4). The $\mu(X)$ vectors are directed toward N_α except for **1** in which case the negligibly small F dipole moment is directed in the opposite direction.

Dative Bond Formation and Electron Density Distribution. It is the variation of these dipole moments together with the population data that allow one to relate the Lewis structures **A/B** and **D/E** with the electron density functions. Beginning with **D** (or **E**), **A** (or **B**) results by engaging the N_α lone pair in an additional bond. The more important **A** (or **B**) becomes the more should the asymmetry of the N_α basin deviate from that of N in N_2 in such a way as to increase the electron density in the X–N bonding region. The important point is that this density shift may be reflected in the topological analysis in *either of two ways*. In the initial phase of increasing importance of **A** (or **B**) (such as in the

(46) N in N_2 has an atomic dipole moment of 0.612 au directed toward the bonding region at the RHF/6-31G* level.

Table IV. Charge and Dipole Progression along the N–O Bond Formation Path in **2**

NO	N-charges			N-dipoles				energies			
	N_α	N_β	N_2	$\mu(N_\alpha)$	angle	$\mu(N_\beta)$	angle	$E(N_\alpha)$	$E(N_\beta)$	$E(N_2)$	$E(RHF)$
1.27	−0.145	+0.881	0.736	0.822	172.5	1.059	0.1	−54.896 73	−53.688 76	−108.585 49	−183.916 21
1.50	−0.121	+0.703	0.582	0.297	164.0	0.886	0.4	−54.711 59	−53.976 40	−108.687 99	−183.889 83
1.75	−0.119	+0.531	0.412	0.106	36.6	0.773	0.5	−54.611 84	−54.147 36	−108.759 20	−183.851 92
2.00	−0.137	+0.400	0.263	0.333	8.2	0.712	0.4	−54.575 59	−54.245 64	−108.821 23	−183.824 46
2.25	−0.146	+0.300	0.154	0.493	3.8	0.674	0.4	−54.559 67	−54.308 11	−108.867 78	−183.806 48
2.50	−0.143	+0.226	0.083	0.588	1.9	0.651	0.2	−54.549 16	−54.350 87	−108.900 03	−183.794 79

**Table V.** Variation in Topological Properties of **2** as a Function of the N–O Bond Length[a]

NO bond	topological properties							
	r_A	r_B	F	ρ	λ_1	λ_2	λ_3	ϵ
1.27	0.660	0.414	0.614	0.651	−1.412	−1.308	0.456	0.079
	0.647	0.622	0.510	0.440	−1.075	−0.957	1.147	0.124
1.50	0.608	0.466	0.566	0.669	−1.454	−1.428	0.379	0.018
	0.806	0.694	0.537	0.245	−0.516	−0.449	0.868	0.149
1.75	0.576	0.498	0.536	0.683	−1.512	−1.505	0.508	0.005
	0.953	0.797	0.545	0.123	−0.227	−0.191	0.625	0.185
2.00	0.561	0.513	0.522	0.693	−1.564	−1.562	0.556	0.002
	1.093	0.907	0.547	0.061	−0.095	−0.076	0.378	0.242
2.25	0.552	0.522	0.514	0.701	−1.609	−1.607	0.577	0.001
	1.237	1.014	0.550	0.032	−0.041	−0.032	0.199	0.307
2.50	0.546	0.528	0.508	0.706	−1.643	−1.643	0.591	0.000
	1.385	1.118	0.553	0.017	−0.019	−0.014	0.100	0.365

[a] First entry for N_α–N_β bond; second entry for N_α–O bond. [b] Compare legend to Table I.

alkyldiazonium ions), a change in the asymmetry of the N_α basin (dipoles) is observed while the increasing importance of **A** (or **B**) is not yet manifested in the charge transfer (charges). Only as **A** (or **B**) becomes more and more important will a manifestation in the populations as well be observed.

The principal point can be made by considering a system X–V in which the electronegativity of X is varied from X = U where EN(U) < EN(V) via X = V to X = W with EN(W) > EN(V).
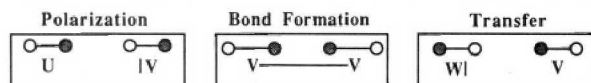
Initially the lone pair at V will only be polarized toward the electron deficient atom U with its dipole moment (generally of different magnitude) aligned in a parallel fashion. In the case where X = V, the electron pair is shared and the increased atomic dipoles become aligned in an antiparallel fashion. Finally, in the case of X = W, the pair is transferred completely and the dipole moments are reversed compared to the U–V scenario.

As a concrete example of charge and dipole variations in the course of bond formation, we studied the electronic relaxation along the reaction path for the association of N_2 with HO^+ leading to **2**. The N_2 group assumes the role of the donor V and the reduction in the N–O bond distance allows one to control the degree by which the "N_α lone pair" is transferred toward X. Several structures of **2** with N–O bond lengths between 2.5 Å and the equilibrium bond length were optimized and their integrated and topological properties are summarized in Tables IV and V, respectively. At $d(N-O)$ = 2.5 Å, the N charges indicate the expected internal N_2 polarization. The charge transfer from N_2 to HO^+ is still marginal (0.08) and the dipole moments of the N atoms are directed as in free N_2 with modest changes in magnitude. This scenario closely resembles that of **4** (only with a smaller degree of internal N_2 polarization). Shortening of the N–O bond results in a steady increase of the N_β and N_2 charges and a comparatively *small* effect of the N_α charge (Figure 5). To the contrary, the dipole moment of N_β is affected comparatively little while $\mu(N_\alpha)$ varies *greatly* with the N–O distance. At an N–O distance of about 1.65 Å, $\mu(N_\alpha)$ changes its direction, and at that point of the reaction path about one-half of an electron has been transferred.

The relation between the characteristics of the electron density functions are expressed in the topological and integrated properties
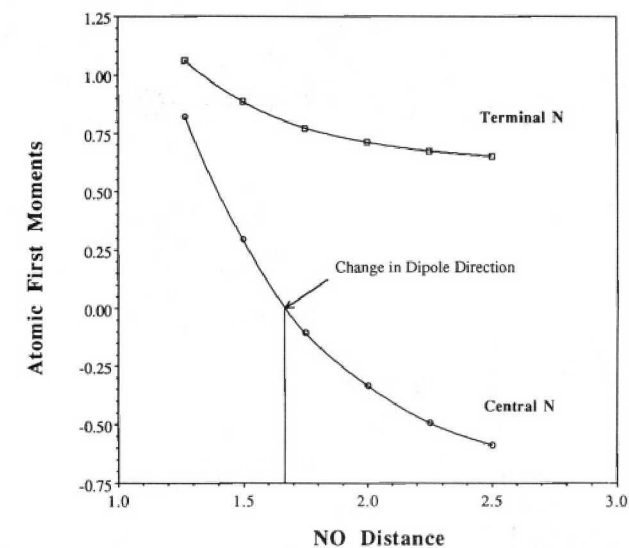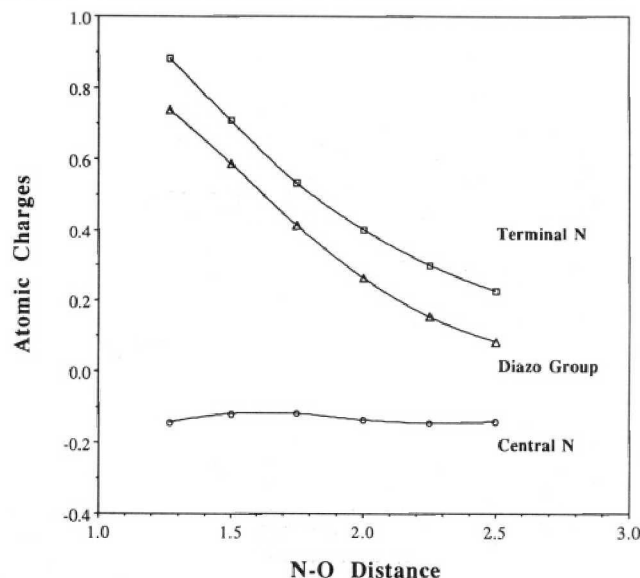
Figure 5. Variation of the atomic charges (left) and dipole moments of N_α (circles) and N_β (squares) in **2** as a function of the O–N distance. The N_β dipoles always point toward N_α, and the N_α dipoles are taken positive if they point away N_β (parallel to $\mu(N_\beta)$), and negative otherwise.

of X and N_β with the valence bond description becomes straightforward. The behavior of the X populations and of the atomic dipoles of X in dependence of the X electronegativity are typical for dative bond formation between X^+ and the donor N_2, and they reflect fully the increasing importance of **A** and **B** and the decreasing importance of **D** and **E** with increasing X electronegativity. The charge increase and the relative constancy of the dipole moment of N_β with increasing electronegativity of X are typical for any homonuclear bond in which the electronegativity of one atom (N_α) is altered moderately by an attached substituent (X). Resonance forms **B** and **E** are important to describe the electronic situation of N_β.

Most importantly, we can now reconcile the dilemma stated above regarding the Lewis structures **A/B** and **D/E** with the

consideration of both the charges *and* the dipole moments of N_α. The initial phase of a dative bond formation is characterized by an increase in the anisotropy of the electron density distribution within the donor basin, and *this change in the asymmetry of electron density is manifested in the atomic dipole moment while it might have little effect on the atomic charge.* The N_α dipole moment in **4** is drastically reduced in magnitude compared to free N_2 and indicates a polarization of N_α electron density into the C–N bonding region. That is, *the notations A and B are useful in the sense that they indicate the direction of the polarization so long as it is kept in mind that this polarization does not cause a full charge transfer.* The topological properties of N_α in the heterodiazonium ions are interpreted more easily because X–N bond formation is more progressed, and, in this stage of bond formation, it is indeed reflected in the atomic charges.

The significance of the atom anisotropies for the description of the electronic structures points up an important and general advantage of the topological method over the basis set partitioning methods. While all techniques provide populations to describe the *polarity of bonds*, only the topological method provides for atomic dipole moments and, thus, for the examination of the *polarity of atoms*. In dative bond formations the latter is especially crucial as the bond formation in the initial stage is characterized by large anisotropies in the donor atom and comparatively little charge transfer to the acceptor.

Atom Anisotropy and Correlation Effects on Electron Density Distributions. The atomic dipole moments are important for the correct interpretation of the effects of electron correlation on the electron density distribution and the derived atomic properties. The electron correlation effects on the integrated N populations (Figure 2) are large, but to conclude from this finding that electron correlation also has a large effect on the bonding would be simplistic. The large population changes result from large changes in the atomic volumes which are fully reflected in volume-dependent parameters such as the atomic dipoles. Large changes in the integrated properties of the individual atoms do not necessarily mean that the electron density distribution in the bonding regions has changed drastically, and, moreover, the theory of atoms in molecules is quite capable to support this argument so long as charges *and* dipole moments of atoms are discussed instead of just atomic charges alone.[47] The point is perfectly made by considering the effects of electron correlation on the integrated properties of N_α and N_β. Note that the effects on the entire diazo group are rather small in all cases. Electron correlation increases (reduces) the population of N_β (N_α), and the primary reason for this change is a *small* effect of electron correlation on the curvature of the electron density in the N–N bonding region which causes a disproportionately *large* increase (reduction) of the atomic volume of N_β (N_α) since the λ_3 values in triple bonds are comparatively small in general. The volume increase of the N_β basin in the N–N

bonding region by itself will reduce the N_β dipole moment. Similarly, the concomitant decrease of the N_α basin in that region by itself will increase or reduce the magnitude of the N_α dipole depending on whether the N_α moment is oriented antiparallel (X = alkyl) or parallel (X = F, OH, NH_2) with regard to the N_β dipole, respectively. The changes of the integrated charges together with changes of the dipole moments show that the integrated properties might be affected dramatically by modest changes in the electron density function itself. To correctly appreciate electron correlation effects on the basis of integrated properties, it thus seems mandated that the correlation effect on another volume-dependent parameter, such as the dipole moment, be considered at the same time. Furthermore, this discussion emphasizes the benefits of envisioning the electron correlation effects graphically via plots of the type shown in Figure 1.

Conclusion

An analysis has been presented of the electron density distributions of heterosubstituted diazonium ions **1 – 4** and of the changes in atom populations and atom anisotropies that accompany progressing X–N bond formation. Dative bonding may be reflected in the topological analysis in *either of two ways.* Weak dative bonding is characterized primarily by an increase in the anisotropy of the donor basin, while stronger dative bond formation finds its manifestation in the population changes associated with charge transfer. Both atom populations *and* atom dipole moments are equally significant for the description of dative bond formation.

The electronic structures of **1 – 4** are inconsistent with the commonly used Lewis structure **A** *as the single representation.* While **A** assigns a positive charge to N_α, this work shows that the positive charge on N_β is always larger than the one on N_α and that N_α might even carry a negative charge. The X–N nonconnected Lewis structures **D** and **E** need to be considered for the adequate representation of the electron density distributions in **1–4.** Our results suggest that a combination of **D** and **E** best represents alkyldiazonium ions in terms of atom charges, but the Lewis structures **A** and **B** are useful and required in the sense that they indicate the direction of the donor basins's polarization and the accumulation of electron density in the X–N bond. As the X–N_α bond strengthens with increasing electronegativity of X, **A** and **B** become more important. In general, the Lewis structures that reflect the $N_\alpha{}^{\delta-}$–$N_\beta{}^{\delta+}$ type polarization, **B** and **E**, contribute *more than A and D. Alkyldiazonium ions and their heteroderivatives differ significantly in that the former essentially are carbenium ions, whereas the latter are diazonium ions with larger positive charges on the terminal nitrogen atom.*

---

(47) Although the atomic charges and atomic dipoles vary significantly with the theoretical model, the electrostatic properties of the molecules (cf. dipole moments in Table III) are affected little, reflecting the modest effects of electron correlation on the electron density distributions. Note that the integrated charges and atomic first moments together exactly reproduce the directly computed molecular dipole moments.